Published in final edited form as:

Cell Calcium. 2010 July ; 48(1): 28–36. doi:10.1016/j.ceca.2010.06.003.

Altered calcium pump and secondary deficiency of γ-sarcoglycan and microspan in sarcoplasmic reticulum membranes isolated from δ-sarcoglycan knockout mice

Alhondra Solares-Pérez[a,b,c], **Rocío Álvarez**[d], **Rachelle H. Crosbie**[e], **Jesús Vega-Moreno**[d], **Joel Medina-Monares**[d], **Francisco J. Estrada**[f], **Alicia Ortega**[d,g,*], and **Ramón Coral-Vazquez**[a,b,c,**]

[a]Sección de Posgrado, Escuela Superior de Medicina, Instituto Politécnico Nacional, México, DF., México

[b]División de Medicina Genómica, Subdirección de Enseñanza e Investigación, Centro Médico Nacional 20 de Noviembre, Instituto de Seguridad y Servicios Sociales de los Trabajadores del Estado, México, D.F., México

[c]Unidad de Investigación Médica en Genética Humana, Hospital de Pediatría, Centro Médico Nacional Siglo XXI-IMSS, México, D.F., México

[d]Departamento de Bioquímica, Facultad de Medicina, Universidad Nacional Autónoma de México, México, D.F., México

[e]Department of Physiological Science and the Molecular Biology Institute, University of California, Los Angeles, CA, USA

[f]Laboratorio de Biología Molecular, Escuela de Medicina, Universidad Panamericana, México, D.F., México

[g]Departamento de Bioquímica, Instituto Nacional de Perinatología, México, D.F., México

Abstract

Sarcoglycans (SGs) and sarcospan (SSPN) are transmembrane proteins of the dystrophin-glycoprotein complex. Mutations in the genes encoding SGs cause many inherited forms of muscular dystrophy. In this study, using purified membranes of wild-type (WT) and δ-SG knockout (KO) mice, we found the specific localization of the SG-SSPN isoforms in transverse tubules (TT) and sarcoplasmic reticulum (SR) membranes. Immunoblotting revealed that the absence of δ-SG isoforms in TT and SR results in a secondary deficiency of γ-SG and μSPN. Our results showed augmented ATP hydrolytic activity, ATP-dependent calcium uptake and passive calcium efflux, probably through SERCA1 in KO compared to WT mice. Furthermore, we found a conformational change in SERCA1 isolated from KO muscle as demonstrated by calorimetric

*Corresponding author at: Departamento de Bioquímica y Biología Molecular, Facultad de Medicina, Universidad Nacional Autónoma de México, Av. Universidad 3000, C.P. 04510AP 70-159, México, D.F., México. Tel.: +52 55 56232511; fax: +52 55 56162419, aortega@unam.mx (A. Ortega). **Corresponding author at: Sección de Posgrado, Escuela Superior de Medicina Plan de San Luis y Díaz Mirón s/n, Col. Casco de Santo Tomas, México; División de Medicina Genómica, Subdirección de Enseñanza e Investigación, San Lorenzo No 502-2° piso, Col Del Valle, Delegación Benito Juárez, C.P. 03100, México, D.F., México. Tel.: +52 55 57296300x16820/55755306; fax: +52 55 57296300x16820/55755306. rmcoralv@gmail.com (R. Coral-Vazquez).

analysis. Following these alterations with mechanical properties, we found an increase in force in KO muscle with the same rate of fatigue but with a decreased fatigue recovery compared to WT. Together our observations suggest, for the first time, that the δ-SG isoforms may stabilize the expression of γ-SG and μSPN in the TT and SR membranes and that this possible complex may play a role in the maintenance of a stable level of resting cytosolic calcium concentration in skeletal muscle.

Keywords

Muscular dystrophy; Calcium; Sarcoglycans; Skeletal muscle; SERCA1; Sarcoplasmic reticulum; δ-Sarcoglycan; Microspan; Knockout; Pathology

1. Introduction

The dystrophin-glycoprotein complex (DGC) is a multimeric assembly composed of transmembrane and membrane-associated proteins that connect the extracellular matrix with the cytoskeleton of the muscle fiber [1].The function of this complex appears to include protection against contraction-induced damage. Data also support a possible role in cell signaling pathways [1,2]. Mutations in genes encoding components of the DGC cause several forms of muscular dystrophy. The pattern of inheritance may be X-linked recessive as in Duchenne or Becker muscular dystrophy or autosomal dominant as in limb-girdle muscular dystrophy type 1 or autosomal recessive as in limb-girdle muscular dystrophy type 2 [3–5]. The DGC consists of the dystroglycan subcomplex, SG-SSPN subcomplex and the cytoplasmic subcomplex [6,7]. The SG-SSPN subcomplex is composed of α, β, γ, and δ-SGs and SSPN [8]. A fifth member of the sarcoglycan family, ε-SG, is closely related to α-SG, and both are co-expressed in striated muscle as part of a biochemically distinct complex [9,10]. The SG-SSPN subcomplex of sarcolemma is thought to stabilize α- and β-dystroglycan interaction as well as dystrophin and β-dystroglycan interaction [11].

Each of the SGs proteins has a short intracellular domain, a single transmembrane domain and a large extracellular domain with multiple predicted N-glycosylation sites and cysteine residues that are conserved across species [12]. The heteromeric SG subcomplex assembles early in the secretory pathway around a β/δ-sarcoglycan core. Loss of δ-SG leads to complete absence of α-, β-, γ-, and ε-SG, despite normal levels of transcription. In contrast, a mutation in γ-SG reduced but did not eliminate expression of α-, β-, δ- and ε-SG [13]. The localization of SGs was thought to be exclusively at the sarcolemma membrane until electron microscopy revealed that δ-SG, δ-SG3 and γ-SG are located at the SR membrane independent of dystrophin expression [14,15]. We have identified an isoform of δ-SG (δ-SG3) that originates from alternative splicing of the δ-SG transcript and has 10 new amino acids at its C-terminus that replace the last 122 amino acids of δ-SG [15]. Crosbie and colleagues recently reported that alternative splicing of SSPN transcripts produces microspan (μSPN), which is composed of two transmembrane domains and a novel C-terminal region [16]. Biochemical analysis revealed that μSPN is not associated with the DGC at the sarcolemma, and its expression is not affected by the loss of dystrophin. Rather, μSPN is localized within SR membranes. Forced overexpression of μSPN results in

morphological abnormalities in SR-TT structures detected by the presence of small triads that were misaligned within the sarcomere as well as an overall decrease in the number of triads in skeletal muscle [16].

In the present study we purified skeletal muscle membranes from WT and δ-SG KO mice and determined the expression of δ-SG and its isoforms, γ-SG and μSPN, in TT and SR fractions. Furthermore, we examined the functional and structural conformation of the calcium pump (SERCA1) in WT and δ-SG KO mice. We provided evidence for distorted structural conformation and function of SERCA1 in δ-SG KO mice, suggesting that the SGs and μSPN present in SR may play a role in SERCA1 structure and function in addition to contributing to dysregulation of cytosolic calcium in dystrophy. Our results, using complete muscles, demonstrated alterations in the mechanical properties of KO muscle compared to WT, suggesting that absence of this alternative complex has consequences in the whole muscle, contributing to the pathogenesis of muscular dystrophy.

2. Materials and methods

2.1. Animals

All procedures were conducted in accordance with the U.S. Guidelines for the Care and Use of Laboratory Animals of the Institute of Laboratory Animal Resources as approved in Mexico by the National Academy of Medicine (http://www.nal.usda.gov/awic/pubs/noawicpubs/careuse.htm). WT and δ-SG KO (δ-sarcoglycan null B6.129-*Sgcd*^{tm1Mcn}/J) mice were purchased from the Jackson Laboratory (Bar Harbor, ME). The genotype of the δ-sarcoglycan locus was determined using a protocol provided by the Jackson Laboratory to differentiate between WT and δ-SG KO mice (http://jaxmice.jax.org/strain/004582.html).

2.2. Isolation of TT and SR membranes

TT and SR membranes were obtained from the fast skeletal muscle (forelimbs, hindlimbs and back muscles) of 4-month-old WT and δ-SG KO mice. Fifty WT and 50 δ-SG KO mice were used for each preparation. Isolation was performed by differential centrifugation and a discontinuous sucrose gradient as previously described [17]. Membrane isolation was performed in the absence of any reducing agent in the buffer medium. The microsomal fraction was placed in a first sucrose gradient of 25%, 27.5%, and 35% (w/v). The 25/27.5% interface showed the maximal signal for DHPR as determined by immunoblotting, indicating that it corresponded to TT membranes. When required, isolated TT membranes were incubated in a Ca^{2+} loading solution in the presence of 5 mM potassium oxalate. An additional centrifugation through a 25/45% discontinuous sucrose gradient was done to remove Ca^{2+}-oxalate-loaded vesicles [18]. Heavy SR (HSR) and light SR (LSR) were isolated from the 35% band obtained from the first discontinuous sucrose gradient essentially as previously described [19]. LSR was detected by the maximum ATPase activity stimulated by Ca^{2+} and HSR was detected by the maximal immunoreactivity with the antibody anti-RyR. Protein concentration was determined using Coomassie Plus Protein Assay Reagent (Pierce, Rockford, IL, USA) with BSA as the standard.

2.3. Immunoblotting

Protein samples were subjected to 4–20% SDS PAGE (Pierce) and transferred to nitrocellulose membranes (Millipore, Bedford, MA, USA). Immunoblotting was performed using the following antibodies: NCL-g-SARC (γ-SG) purchased from Novocastra. Antibody to SERCA-1 was obtained from Affinity BioReagents. β-DG, DHPR (IIID5E1) and RyR (C34) antibodies were obtained from the Iowa Hybridoma Facility. Triadin (GE 4.90), calsequestrin (VIIID12) and C-terminal delta sarcoglycan (δ-SG) were obtained from Abcam. Antibody to δ-SG3 and μSPN (R13) were described previously [15,16]. All immunoblots were developed using enhanced chemiluminescence (Pierce).

2.4. Calcium uptake

Calcium transport was measured at room temperature (25 °C) by the filtration method with LSR aliquots in a solution containing the following (in mM): 100 KCl, 5 $MgCl_2$, 0.1 $CaCl_2$, 1 μCi [$^{45}CaCl_2$], 20 Tris–malate (pH 7.0), 5 mM K-oxalate and 4 ATP with 0.15 mg of protein/ml. The reaction was stopped with 0.5 ml of ice-cold quenching solution containing the following (in mM): 5 $MgCl_2$, 4 EGTA, and 20 Tris–malate (pH 7.0). Membrane vesicles (0.9 ml) were filtered through 0.45-μm Millipore filters, washed, dried, and then counted by scintillation. Experiments were done in isolated LSR from WT mice muscle and δ-SG KO mice. All values are expressed as mean ± standard deviation (SD).

2.5. Passive Ca^{2+} efflux from LSR

ATP-dependent Ca^{2+}-loading in vesicles was done for 30 min with LSR aliquots in a solution containing the following (in mM): 0.1$CaCl_2$, 5 $MgCl_2$, 100 KCl, 20 Tris–malate, 1 Mg-ATP, 1 μCi [$^{45}CaCl_2$], pH 7.0, at a concentration of 300 μg protein/ml in the absence of K-oxalate. Vesicles were then diluted in a solution containing 2 mM EGTA. The amount of $^{45}Ca^{2+}$ remaining in the LSR vesicles was determined by filtration and its radioactivity was measured with a scintillation counter. For the SERCA1 inhibition experiment, 2.5 μM of thapsigargin (Sigma) was used.

2.6. SERCA1 hydrolytic activity

Total ATPase activity was measured by colorimetric determination of P_i using malachite green as previously described [20]. Aliquots of 5 μg/ml of protein were incubated in a solution containing the following (in mM): 100 KCl, 5 $MgCl_2$, 5 NaN_3, 1 ouabain, 0.1 $CaCl_2$, 0.33 ATP and 20 Tris–malate, pH 7. The reaction was stopped with a solution containing 0.045% malachite green hydrochloride, 4.2% ammonium molybdate in 4N HCl, 0.8 ml Triton-X 100 for each 100 ml of solution, and 0.25 ml Na-citrate (34%). Absorbance was read at 660 nm. For the Ca^{2+} ATPase (SERCA1) inhibition experiment, 500 nM of thapsigargin (Sigma) was used.

2.7. Differential scanning calorimetry (DSC)

DSC was used to measure the transition temperature (T_m) of SERCA1 isolated from WT and δ-SG KO mice muscles. T_m is defined as the temperature at which excess heat capacity is maximal. LSR was dissolved in a buffer containing (in mM) 100 KCl and 20 Tris–malate (pH 7.0). Excess heat (Cp) vs. temperature scans were obtained from ~1 mg/ml protein

using a high-sensitivity differential scanning calorimeter VP-DSC (MicroCal Inc., MA, USA). The samples and reference solutions were carefully degassed under vacuum for 5 min before fully loading the DSC containers with a capacity of 0.56 ml. After reaching equilibrium at 10 °C, the temperature was increased to 100 °C. Each scan was performed at the rate of 1 °C/min. To assess for protein denaturation reversibility, the temperature was cooled down to 10 °C and rescanned to 100 °C. The baseline was corrected by subtracting the rescan from the scan. There was no evidence of reversibility in any of the cases. DSC profiles were deconvoluted and the best theoretical fit was calculated assuming irreversible denaturation as previously described for SR [20,21]. All values were expressed as mean ± standard error of the mean (S.E.M.).

2.8. Muscle preparation

WT and δ-SG KO mice aged ~4 to 6 months were euthanized by cervical dislocation followed by isolation of the *extensor digitorum longus* (EDL) at room temperature. The isolated muscle was placed in an acrylic chamber equipped with platinum electrodes all along each side of the chamber wall. We used Krebs solution (135 mM NaCl, 5 mM KCl, 1 mM $MgCl_2$, 2.5 mM $CaCl_2$, 11 mM dextrose, 1 mM $NaPO_4$ dibasic, 15 mM $NaHCO_3$) bubbled with 95% O_2 and 5% CO_2 to reach pH 7.0. EDL muscle was fastened by the distal tendon with a forceps and the proximal tendon with a force transducer. Platinum electrodes were connected in parallel to two stimulators (Grass SD9).

2.9. Mechanical protocol

Single electrical pulses of 0.6 ms were used to reach the maximal voltage for the maximal tension. Muscles were stretched to the optimal length for maximal twitch force. Tetanic stimulation of 75 Hz for 5 s was used followed by a 3-min rest. This protocol was repeated several times with 3-min resting periods to ensure that at least three control-tetanic forces were repeated. This force was considered the control maximal tetanic-tension. At the end of the protocol, the muscle rested for 10 min before the fatigue protocol began.

2.10. Fatigue and fatigue recovery protocols

Fatigue was induced with cycles of tetanic stimulation that consisted of a 0.6-s long train of electrical stimulation at 75 Hz, 100 V applied for 70 s (Fig. 6A, fatigue). After fatigue protocol, the muscle rested for 5 min and a new protocol of tetanic stimulation showed muscle recovery tension. The stimulation was repeated at least 5 times, every 5 min, to see fatigue recovery (Fig. 6A, recovery). Muscle force (mN) was determined using a calibration mass curve (Fig. 5).

3. Results

3.1. Biochemical localization of δ-SG isoforms, γ-SG and μSPN in TT and SR membranes

Isolated TT, LSR and HSR membranes were prepared from skeletal muscle of WT and δ-SG KO mice and separated by sucrose gradient ultracentrifugation. In order to determine the purity of isolated vesicles, we performed immunoblot analyses on isolated membranes with the appropriate antibody markers. We show that (1) β-DG was detected only in a small amount in TT membranes from δ-SG KO mice. Because the loss of δ-SG leads to the

complete absence of the other sarcoglycans [13], we did not detect any sarcoglycan contamination, (2) DHPR was enriched in TT fractions and was not detected in the SR membranes, (3) RyR was detected only in the HSR and (4) SERCA1 was detected in both SR fractions although low levels were present in HSR (Fig. 1A). Isolated membranes from WT and KO mice were analyzed by immunoblotting with antibodies to δ-SG, γ-SG, δ-SG3 and μSPN. The TT membranes are finger-like invaginations of the sarcolemma that are typically located at the level of the A-I junction around the myofibrils. Skeletal muscle utilizes the TT system that contains a large number of L-type calcium channels (DHPR) to provide a uniform contraction [22]. Interestingly δ-SG and γ-SG were detected in the TT fraction of WT mice but were absent from the TT of dystrophic mice (Fig. 1B). TT membranes are structurally and functionally associated with the SR and intracellular calcium stores [23]. SR is segregated into two functional domains, a longitudinal part (LSR) with SERCA1 enrichment and a junctional part (HSR) composed of terminal cisternae, which are adjacent to each TT [22] and contain proteins such as RyR, triadin and calsequestrin [23]. Fig. 1C shows the purified LSR membranes. We found that δ-SG, δ-SG3, γ-SG and μSPN were enriched in WT mice but absent from LSR of δ-SG KO mice. Fig. 1D shows the HSR membranes in which we found that δ-SG3 was present in WT mice but absent from HSR of dystrophic mice. μSPN was present in WT mice but was severely reduced in δ-SG KO mice. Triadin and calsequestrin appear slightly decreased in δ-SG KO mice compared to levels in WT mice.

3.2. Calcium uptake and passive calcium efflux are augmented in LSR of δ-SG KO mice

We performed calcium release and uptake experiments with HSR and LSR vesicles obtained from WT and δ-SG KO skeletal muscle. Differences in Ca^{2+} release were not observed in isolated HSR vesicles from WT and δ-SG KO animals (data not shown). In contrast, passive Ca^{2+} efflux and uptake was notably affected in LSR vesicles of δ-SG KO mice compared with WT animals. Fig. 2A shows that the ATP-dependent Ca^{2+} transport by LSR from δ-SG KO muscles increased 2-fold relative to WT controls after a 30-min reaction. Ca^{2+} transport at 30 min increased from 84 ±7 to 160±18 nmol/mg protein ($n = 3$). Fig. 2B shows the normalized passive Ca^{2+}-efflux activity. The normalized activities of calcium efflux measured 30 min after the beginning of the reaction were 30% and 90% for WT and δ-SG KO muscles, respectively. To investigate whether SERCA1 may be involved in the passive calcium efflux, we used the SERCA1-specific inhibitor thapsigargin. Thapsigargin inhibits the passive efflux of calcium in WT by 14%, whereas in the KO there is an inhibition of 83%, leaving the total passive calcium efflux from LSR equivalent in both muscles in the presence of the inhibitor. This result suggests that SERCA1 is involved in passive Ca^{2+} efflux (Fig. 2B).

3.3. Ca^{2+} pump hydrolytic activity is augmented in LSR of δ-SG KO mice

In skeletal muscle during muscle activation, Ca^{2+} release from the SR produces actomyosin interaction and contraction. On the other hand, reuptake of calcium by SERCA1 lowers the intracellular calcium concentration to a resting level, producing relaxation [20]. To compare the SR pump ATP hydrolytic activity of WT and δ-SG KO mice, we measured the activity of SERCA1 30 min after the onset of the hydrolytic reaction (Fig. 3) (see Section 2). We found that the ATP hydrolytic activity in LSR vesicles was 7.64 μmol P_i/mg of protein for WT

mice and 12.42 μmol P_i/mg of protein for δ-SG KO. Hydrolytic activity was 1.6-fold higher in δ-SG KO vesicles relative to WT. Thapsigargin inhibited the time course of the ATP hydrolytic activity of SERCA1 with 75% and 65% inhibition at 30 min for the WT and KO, respectively (Fig. 3).

3.4. Differential scanning calorimetry

To investigate whether the deficiency of δ-SG isoforms induced conformational changes in SR membrane proteins, we used DSC to investigate the denaturation profile of LSR membranes from WT and δ-SG KO mice. In our studies, isolated LSR membranes showed important changes in the protein denaturation profile of dystrophic mice compared with control animals. The T_m and enthalpy (heat of transition) of Ca^{2+} pumps indicated a change in the native structure of the proteins. Denaturation profiles obtained from a heating rate of 1 °C/min mainly showed denaturation of the Ca^{2+} pump. The protein electrophoretic pattern of LSR used in these experiments revealed an 80–90% composition of Ca^{2+} pump. Lepock et al. [21] demonstrated that, in the presence of 1 mM $CaCl_2$, two different transitions, *A* and *B*, appear in the DSC profile. *Transition A* corresponded to the denaturation of the nucleotide-binding domain (NBD), and *transition B* corresponded to the denaturation of the transmembrane Ca^{2+}-binding domain (CBD) [21,24]. Several pieces of evidence demonstrated that conformational changes in SERCA1 induced by the presence of SERCA1 inhibitors such as the calcium channel blocker D-600 [24] or redox modification through SERCA1 vicinal thiol oxidation [25] and biological conditions that modify SERCA1 activity such as changes during muscle fatigue or muscle adaptation to exercise [25,26] are reflected by changes in the SERCA1 conformations revealed by modification on the SERCA1 thermodynamic parameters obtained from thermal denaturation (DSC). Fig. 4 shows the DSC profile of LSR membranes isolated from muscles of control (*A*) and δ-SG KO (*B*) mice. In the control mice profile we detected two transitions, T_m (NBD) 49 ± 1.3 °C (n = 3) and T_m (CBD) 61.7 ± 1.02 °C (n =3) (Fig. 4A). In the δ-SG KO mice profile, we detected four transitions, T_m (NBD) 50.5 ± 1.03 °C (n = 3), T_m (CDB) 66.6 ± 0.58 °C (n = 3), and two new transitions that we referred to as undetermined domains (UD) with T_m (UD1) 40 ± 0.33 °C (n =3) and Tm (UD2) 56.6 ± 0.33 that are only present in the profile of the dystrophic mice (Fig. 4B).

3.5. Mechanical properties of WT and δ-SG KO muscles

Isolated EDL muscles from WT and δ-SG KO mice were examined with the mechanical protocol as described previously in Section 2. Fig. 5 shows the tetani resulting from three consecutive stimulations. Fig. 5A correspond to the WT and Fig. 5B to the δ-SG KO muscle stimulations. Using the recordings, we calculated an initial force of 259 and 236 mN for the WT and the δSG KO, respectively. In the case of WT, we found a decrease in force in each tetanus on average of 27 mN and a decrease in tension between the first and the third tetanus of 112 mN. This represents a 40% loss of force of the original tension, which reversed after a period of rest. In the δ-SG KO muscle, in each tetanus there was an average increase in force of 54.5 mN and the tension between the first and the third tetanus was 14mN, representing a decrease in force of 9.5%.

In Fig. 6A we show a representative experiment of fatigue obtained after tetanic stimulation to produce up to 30% of the original force (fatigue protocol) and the recovery of force after rest. Fig. 6B shows the normalized force in the fatigue experiment for WT and the δ-SG KO (n = 3). Loss of 70% of force in both muscles was achieved at the same time (70 s) and was 77mN for WT and 67 mN for δ-SG KO mice, without a significant difference. Fig. 6C shows the representation of the percentage of recovery after the fatigue protocol. At 5 min the WT recovery was 70% and 55% for the KO, with the maximal recovery force at 20 min with 89% recovery for the WT mice. In KO mice, at the same time there was a decrease in force of recovery of only 46%. In WT mice we observed an increase in force during recovery that provides evidence of the fatigue phenomenon. In the δ-SG KO there was a partial recovery with a significant drop of force after consecutive stimulation, proving the irreversible damage of muscle cells.

4. Discussion

4.1. Localization of δ-SG isoforms, γ-SG and μSPN in calcium regulatory membranes

Muscle fibers have specialized protein complexes in the plasma membrane that protect against contraction-induced damage and may additionally play a role in cell signaling pathways [1,2]. The SG-SSPN subcomplex forms part of the DGC in sarcolemma and defects in the genes encoding the components of this subcomplex produce many forms of limb-girdle muscular dystrophy and in some cases dilated cardiomyopathy [4,27]. The SG complex is assembled from a core composed of β and δ-SG. Loss of δ-SG leads to complete absence of the other sarcoglycans. In contrast, a mutation in γ-SG reduced, but did not eliminate, expression of α-, β-, δ- and ε-SG [13,11]. Interestingly, SGs are not only located in the sarcolemma of the muscle fibers. We previously reported the identification of δ-SG3 [15]. Other investigators reported the localization of δ-SG, γ-SG [14] and μSPN [16] in SR membranes.

In this study, immunoblot analysis of purified membranes from WT mice revealed that δ-SG and γ-SG are enriched in TT membranes. We also show that δ-SG, γ-SG, δ-SG3 and μSPN are present at low levels in purified LSR fractions, whereas δ-SG3 and μSPN are predominantly found in HSR preparations. Recently, Ueda et al. reported that δ-SG was localized in the terminal cisternae of the SR and that γ-SG was found in the longitudinal part and cisternae of the SR [14]. The authors proposed this localization based on microscopy experiments where it is difficult to resolve specific locations of the proteins due to the short distances between TT and the SR cisternae membranes, which range from 9 to 10 nm as determined by electron microscopy [28]. The evidence presented in this paper is based on biochemical analysis of purified membranes, which reveals that δ-SG and γ-SG are present in TT and not in SR cisternae of the muscle fiber. Furthermore, we distinguished between δ-SG isoforms, showing that δ-SG3 is located in the SR cisternae along with μSPN. Interestingly, the TT and SR membranes isolated from skeletal muscle of δ-SG KO mice exhibit a secondary deficiency of δ-SG and μSPN. This phenomenon is similar to that which occurs at sarcolemma in cases of sarcoglycan deficiency [13], suggesting that δ-SG isoforms may serve a similar function as the core protein for the assembly of a homologue SG-SSPN complex in TT and SR. Muscle activation is controlled by the close interactions of two

separate membrane systems, the TT, which are invaginations of the sarcolemma, and the SR, the intracellular calcium store [23]. TT and SR are structurally and functionally joined at Ca^{2+} release units (CRUs). CRUs are the sites at which Ca^{2+} is rapidly released from the SR via the RyRs under control of the DHPR voltage sensor located in the TT [29]. The calcium pump (SERCA1) functions to restore calcium to the SR compartment, thereby terminating muscle contraction [20]. Because these membranes are involved in the regulation of calcium concentration within skeletal muscle, we refer to them as calcium regulatory membranes (CRM). Our results demonstrate that a homologous SG-SSPN complex exists within the CRM, which we will refer to as the CRM SG-SSPN (CRMSS) complex. Currently, this complex is composed of δ-SG isoforms, γ-SG and μSPN. The combination depends on the specific membrane, the TT, the LSR or HSR. For that reason we propose subtypes of this complex ($CRMSS_{TT}$, $CRMSS_{LSR}$ and $CRMSS_{HSR}$) (Fig. 7).

4.2. Effect of the absence of δ-SG isoforms, γ-SG and μSPN in the sarcoplasmic reticulum activity

To explore the function of this alternative complex in the CRM, we performed experiments comparing the SR vesicles of δ-SG KO mice with SR vesicles of WT mice. The results described in this paper show that the SR Ca^{2+} pump of dystrophic animals exhibit the following characteristics compared with WT animals: (1) a considerable increase in passive Ca^{2+} efflux, ATP-dependent calcium uptake and in SERCA1 ATP hydrolytic activity in LSR vesicles compared with controls; (2) a modification in thermal stability and enthalpy of the SR Ca^{2+} pump caused by changes in the Ca^{2+}-binding domain, nucleotide-binding domain and the presence of two new undetermined transitions that are only present in the profile of the dystrophic animals.

The range of passive Ca^{2+} efflux from liposomes of different compositions or from the phospholipids extracted from SR varies from 10^{-15} to 10^{-18} mol/cm^2/s^{-1}, which is several orders of magnitude lower than the passive Ca^{2+} efflux from isolated SR [30]. Therefore, membrane lipids represent the principal permeability barrier to SR Ca^{2+} release. The principal pathway for SR passive Ca^{2+} efflux has been proposed to be through SERCA1. Several lines of evidence have shown that the pump-mediated calcium efflux is Mg^{2+} dependent, requires high intravesicular and low extravesicular [Ca^{2+}], and is inhibited by saturation with Ca^{2+} of the high-affinity Ca^{2+}-binding site of SERCA1 [30,31]. Increased calcium efflux from SR in KO muscles indicates uncoupling of the SERCA1, resulting in an increase of wasted energy to maintain KO muscles at rest. The direct effect of the presence of δ-SG on SERCA1 conformation is under present investigation. Abnormal Ca^{2+}-handling has been described in frequent disorders of skeletal and heart muscle cells [32–34]. In the case of muscular dystrophy, altered calcium homeostasis is a hallmark of muscle dysfunction [35] that has been proposed as an early process initiating activation of Ca^{2+}-dependent proteases [36,37]. Elevation in cytosolic Ca^{2+} concentration beneath the sarcolemma or within other cell compartments in skeletal muscle fibers from dystrophin-deficient Duchenne muscular dystrophy patients and *mdx* mice have been reported [38,39]. Conflicting reports have been published regarding the key Ca^{2+} regulatory membrane proteins in dystrophic skeletal muscle membranes. Previous studies of dystrophin-deficient muscle have shown that the SR Ca^{2+}-ATPase, calsequestrin, the DHPR, and the cytoplasmic

Ca^{2+} binding protein parvalbumin may be affected in the disease process [40–43]. However, Culligan et al. presented evidence that did not reveal any drastic changes in the immunoblotting profile of calsequestrin and DHPR in *mdx* muscle preparations compared with controls. These authors proposed a drastic decline in calsequestrin-like proteins of 150–220 kDa and, analogously, overall Ca^{2+} binding reduction in the SR of dystrophic muscle [44]. In the case of SERCA1 Ca^{2+} pump, previous biochemical analysis suggests that the maximum velocity of Ca^{2+} uptake is impaired in dystrophic *mdx* fibers. The Hill coefficient and Ca^{2+} sensitivity of the Ca^{2+}-ATPase were the same in the SR vesicles derived from skeletal muscle of normal and *mdx* mice. The maximum velocity of Ca^{2+} uptake, however, was less for *mdx* muscle [41]. In contrast, other results showed that neither the relative abundance nor the total enzyme activity of this Ca^{2+} pump protein is altered [44]. Additional abnormalities in the store-operated Ca^{2+} (SOC) channels have been described in *mdx* fibers [45].

In the case of other dystrophic animal models, abnormal Ca^{2+} homeostasis has been reported and studied in cultured myotubes from muscles of BIO 14.6 hamsters, which are deficient in δ-SG. No apparent differences in the levels of expression of various Ca^{2+} handling proteins (DHPR, RyR, SR Ca^{2+} ATPase, and Na^{+}/Ca^{2+} exchanger), muscle-specific proteins (contractile actin and acetyl-choline receptor), or DGC member proteins except SGs and SSPN have been reported [46]. Furthermore, SOC channel abnormalities have been described in the δ-SG KO mouse model [47].

In order to explore whether absence of the CRMSS complexes has an impact on the whole muscle, we analyzed the mechanical properties of WT and δ-SG KO muscle [13] using concentric contraction protocols with tetanic stimulation to achieve fatigue. As previously shown, the twitch and tetanic force generation obtained by eccentric contraction was similar for the control and the dystrophic muscle [13], indicating that the sarcomere and contractile apparatus were intact in the absence of the sarcoglycan complex. Under our experimental conditions, using a concentric contraction protocol, we found an increase in force in δ-SG KO muscle, presumably by an extra calcium efflux from the SR. After a protocol of high-frequency tetanic stimulation, both muscles decreased force up to 30% during the same period of time, suggesting that there is no damage contribution in the myofilaments of δ-SG KO as previously shown with eccentric contraction [13]. However, to demonstrate that the decrease in force is certainly due to fatigue, considering fatigue as a reversible physiological process, we found that recovery of the mechanical properties after fatigue is not achieved in the KO muscle, suggesting cell damage or cell death [13]. Increase in force in the δ-SG KO in concentric tetanic contraction as well as in twitch reported previously [13] indicated an extra availability of calcium in the myofilament space.

In summary, our study provides evidence to support the existence of a novel complex of SGs and μSPN proteins within the CRMs, which we have named the CRMSS complexes. Absence of δ-SG isoforms perturbs the Ca^{2+} pump function and structure and causes altered calcium homeostasis and abnormal mechanical properties after a fatigue protocol in δ-SG KO mice, contributing to the pathogenesis of muscular dystrophy (Fig. 7). Thus, future pharmacological therapeutic approaches will need to be directed to restore calcium homeostasis to suppress muscle degeneration.

Acknowledgments

R.M.C.V. was supported by grants from the Instituto Mexicano del Seguro Social (IMSS) (grant 2006/1A/I/078) and Consejo Nacional de Ciencia y Tecnología (CONACyT) (grant #55199). A.O. was supported by grant #DGAPA-IN227106 and IN227809 from Dirección General del Personal Académico, Universidad Nacional Autónoma de México, and Consejo Nacional de Ciencia y Tecnología (CONACyT) grant #24792. A.S.P. was supported during the Ph.D. program (Programa de Doctorado en Ciencias Biomédicas, Universidad Nacional Autónoma de México) by scholarships from Consejo Nacional de Ciencia y Tecnología, México (#223377), IMSS and Dirección General de Estudios de Postgrado, Instituto de Investigaciones Biomédicas, UNAM.

References

1. Cohn RD, Campbell KP. Molecular basis of muscular dystrophies. Muscle Nerve. 2000; 23:1456–1471. [PubMed: 11003781]
2. Rando TA. The dystrophin-glycoprotein complex, cellular signaling, and the regulation of cell survival in the muscular dystrophies. Muscle Nerve. 2001; 24:1575–1594. [PubMed: 11745966]
3. Ozawa E, Yoshida M, Suzuki A, Mizuno Y, Hagiwara Y, Noguchi S. Dystrophin-associated proteins in muscular dystrophy. Hum. Mol. Genet. 1995; 4:1711–1716. [PubMed: 8541869]
4. Straub V, Campbell KP. Muscular dystrophies and the dystrophin-glycoprotein complex. Curr. Opin. Neurol. 1997; 10:168–175. [PubMed: 9146999]
5. Durbeej M, Campbell KP. Muscular dystrophies involving the dystrophin-glycoprotein complex: an overview of current mouse models. Curr. Opin. Genet. Dev. 2002; 12:349–361. [PubMed: 12076680]
6. Yoshida M, Suzuki A, Yamamoto H, Noguchi S, Mizuno Y, Ozawa E. Dissociation of the complex of dystrophin and its associated proteins into several unique groups by n-octyl beta-d-glucoside. Eur. J. Biochem. 1994; 222:1055–1061. [PubMed: 8026484]
7. Ervasti JM, Sonnemann KJ. Biology of the striated muscle dystrophin-glycoprotein complex. Int. Rev. Cytol. 2008; 265:191–225. [PubMed: 18275889]
8. Crosbie RH, Lebakken CS, Holt KH, et al. Membrane targeting and stabilization of sarcospan is mediated by the sarcoglycan subcomplex. J. Cell Biol. 1999; 145:153–165. [PubMed: 10189375]
9. McNally EM, Ly CT, Kunkel LM. Human epsilon-sarcoglycan is highly related to alpha-sarcoglycan (adhalin), the limb girdle muscular dystrophy 2D gene. FEBS Lett. 1998; 422:27–32. [PubMed: 9475163]
10. Straub V, Ettinger AJ, Durbeej M, et al. Epsilon-sarcoglycan replaces alpha-sarcoglycan in smooth muscle to form a unique dystrophin-glycoprotein complex. J. Biol. Chem. 1999; 274:27989–27996. [PubMed: 10488149]
11. Ozawa E, Mizuno Y, Hagiwara Y, Sasaoka T, Yoshida M. Molecular and cell biology of the sarcoglycan complex. Muscle Nerve. 2005; 32:563–576. [PubMed: 15937871]
12. McNally EM, Duggan D, Gorospe JR, et al. Mutations that disrupt the carboxyl-terminus of gamma-sarcoglycan cause muscular dystrophy. Hum. Mol. Genet. 1996; 5:1841–1847. [PubMed: 8923014]
13. Hack AA, Lam MY, Cordier L, et al. Differential requirement for individual sarcoglycans and dystrophin in the assembly and function of the dystrophin-glycoprotein complex. J. Cell Sci. 2000; 113:2535–2544. [PubMed: 10862711]
14. Ueda H, Ueda K, Baba T, Ohno S. delta- and gamma-Sarcoglycan localization in the sarcoplasmic reticulum of skeletal muscle. J. Histochem. Cytochem. 2001; 49:529–538. [PubMed: 11259456]
15. Estrada FJ, Mornet D, Rosas-Vargas H, et al. A novel isoform of delta-sarcoglycan is localized at the sarcoplasmic reticulum of mouse skeletal muscle. Biochem. Biophys. Res. Commun. 2006; 340:865–871. [PubMed: 16403451]
16. Miller G, Peter AK, Espinoza E, Heighway J, Crosbie RH. Over-expression of microspan, a novel component of the sarcoplasmic reticulum, causes severe muscle pathology with triad abnormalities. J. Muscle Res. Cell Motil. 2006; 27:545–558. [PubMed: 16823602]
17. Rosemblatt M, Hidalgo C, Vergara C, Ikemoto N. Immunological and biochemical properties of transverse tubule membranes isolated from rabbit skeletal muscle. J. Biol. Chem. 1981; 256:8140–8148. [PubMed: 6455421]

18. Sabbadini RA, Okamoto VR. The distribution of ATPase activities in purified transverse tubular membranes. Arch. Biochem. Biophys. 1983; 223:107–119. [PubMed: 6305271]
19. Campbell KP, Franzini-Armstrong C, Shamoo AE. Further characterization of light and heavy sarcoplasmic reticulum vesicles. Identification of the 'sarcoplasmic reticulum feet' associated with heavy sarcoplasmic reticulum vesicles. Biochim. Biophys. Acta. 1980; 602:97–105. [PubMed: 6448074]
20. Ortega A, Alvarez R, Pérez F, Jiménez AM, Gutiérrez JA, Vázquez P. Redox regulation of vicinal dithiol groups of the SERCA1 participates in muscle fatigue. J. Muscle Res. Cell Motil. 2004; 25:597–608. [PubMed: 16118850]
21. Lepock JR, Rodahl AM, Zhang C, Heynen ML, Waters B, Cheng KH. Thermal denaturation of the Ca^{2+}-ATPase of sarcoplasmic reticulum reveals two thermodynamically independent domains. Biochemistry. 1990; 29:681–689. [PubMed: 2140054]
22. Junqueira, LC.; Carneiro, J. Basic Histology, Text and Atlas. 11th. New York: McGraw Hill, Prentice-Hall; 2005. p. 191-194.
23. Takekura H, Flucher BE, Franzini-Armstrong C. Sequential docking, molecular differentiation, and positioning of T-tubule/SR junctions in developing mouse skeletal muscle. Dev. Biol. 2001; 239:204–214. [PubMed: 11784029]
24. Ortega A, Becker VM, Alvarez R, Lepock JR, Gonzalez-Serratos H. Interaction of D-600 with the transmembrane domain of sarcoplasmic reticulum Ca^{2+}-ATPase. Am. J. Physiol. Cell Physiol. 2000; 279:166–172.
25. Alvarez R, Vazquez P, Perez F, Jimenez A, Tirado A, Irles C, Gonzalez-Serratos H, Ortega A. Regulation of fast skeletal muscle activity by SERCA1 vicinal-cysteines. J. Muscle Res. Cell Motil. 2009; 30:5–16. [PubMed: 19115048]
26. Becker V, Gonzalez-Serratos H, Alvarez R, Baermann M, Irles C, Ortega A. Effect of endurance exercise on the Ca^{2+} pumps from transverse tubule and sarcoplasmic reticulum of rabbit skeletal muscle. J. Appl. Physiol. 2004; 97:467–474. [PubMed: 15064299]
27. Coral-Vazquez R, Cohn RD, Moore SA, et al. Disruption of the sarcoglycan-sarcospan complex in vascular smooth muscle: a novel mechanism for cardiomyopathy and muscular dystrophy. Cell. 1999; 98:465–474. [PubMed: 10481911]
28. Suzuki S, Nagayoshi H, Ishino K, Hino N, Sugi H. Ultrastructural organization of the transverse tubules and sarcoplasmic reticulum in a fish sound-producing muscle. J. Electr. Microsc. 2003; 52:337–347.
29. Franzini-Armstrong C, Protasi F. Ryanodine receptors of striated muscles: a complex channel capable of multiple interactions. Physiol. Rev. 1997; 77:699–729. [PubMed: 9234963]
30. Martonosi AN. Mechanisms of Ca^{2+} release from sarcoplasmic reticulum of skeletal muscle. Physiol. Rev. 1984; 64:1240–1320. [PubMed: 6093162]
31. Hasselbach W. The reversibility of the sarcoplasmic reticulum pump. Biochim. Biophys. Acta. 1978; 515:23–53. [PubMed: 147710]
32. Preedy VR, Patel VB, Reilly ME, Richardson PJ, Falkous G, Mantle D. Oxidants, antioxidants and alcohol: implications for skeletal and cardiac muscle. Front. Biosci. 1999; 4:E58–E66. [PubMed: 10430553]
33. Engel, AG.; Yamamoto, M.; Fischbeck, KH. Dystrophinopathies. In: Engel, AG.; Yamamoto, M.; Fischbeck, KM., editors. Myology, Basic and Clinical. 2nd. New York: McGraw-Hill; 1994. p. 1133-1187.
34. Lennon NJ, Ohlendieck K. Impaired Ca^{2+}-sequestration in dilated cardiomyopathy. Int. J. Mol. Med. 2001; 7:131–141. [PubMed: 11172615]
35. Iwata Y, Katanosaka Y, Arai Y, Shigekawa M, Wakabayashi S. Dominant-negative inhibition of Ca^{2+} influx via TRPV2 ameliorates muscular dystrophy in animal models. Hum. Mol. Genet. 2009; 18:824–834. [PubMed: 19050039]
36. Turner PR, Fong PY, Denetclaw WF, Steinhardt RA. Increased calcium influx in dystrophic muscle. J. Cell. Biol. 1991; 115:1701–1712. [PubMed: 1661733]
37. Turner PR, Schultz R, Ganguly B, Steinhardt RA. Proteolysis results in altered leak channel kinetics and elevated free calcium in mdx muscle. J. Membr. Biol. 1993; 133:243–251. [PubMed: 8392585]

38. Mallouk N, Jacquemond V, Allard B. Elevated subsarcolemmal Ca^{2+} in mdx mouse skeletal muscle fibers detected with Ca^{2+}-activated K+ channels. Proc. Natl. Acad. Sci. 2000; 97:4950–4955. [PubMed: 10781103]

39. Robert V, Massimino ML, Tosello V, et al. Alteration in calcium handling at the subcellular level in mdx myotubes. J. Biol. Chem. 2001; 276:4647–4651. [PubMed: 11029464]

40. Gailly P, Hermans E, Octave JN, Gillis JM. Specific increase of genetic expression of parvalbumin in fast skeletal muscles of mdx mice. FEBS Lett. 1993; 326:272–274. [PubMed: 8325378]

41. Kargacin ME, Kargacin GJ. The sarcoplasmic reticulum calcium pump is functionally altered dystrophic muscle. Biochim. Biophys. Acta. 1996; 1290:4–8. [PubMed: 8645705]

42. Niebroj-Dobosz I, Kornguth S, Schutta H, Siegel FL, Hausmanowa-Petrusewicz I. Proteins of muscle subcellular fractions in Duchenne progressive muscular dystrophy stained with “stains-all” cationic carbocyanine dye and coomassie blue. Muscle Nerve. 1989; 12:273–280. [PubMed: 2770780]

43. Pereon Y, Dettbarn C, Navarro J, Noireaud J, Palade PT. Dihydropyridine receptor gene expression in skeletal muscle from mdx and control mice. Biochim. Biophys. Acta. 1997; 1362:201–207. [PubMed: 9540851]

44. Culligan K, Banville N, Dowling P, Ohlendieck K. Drastic reduction of calsequestrin-like proteins and impaired calcium binding in dystrophic mdx muscle. J. Appl. Physiol. 2001; 92:435–445. [PubMed: 11796649]

45. Vandebrouck C, Martin D, Colson-Van Schoor M, Debaix H, Gailly P. Involvement of TRPC in the abnormal calcium influx observed in dystrophic (mdx) mouse skeletal muscle fibers. J. Cell Biol. 2002; 158:1089–1096. [PubMed: 12235126]

46. Iwata Y, Katanosaka Y, Shijun Z, Kobayashi Y, Hanada H, Shigekawa M, Wakabayashi S. Protective effects of Ca^{2+} handling drugs against abnormal Ca^{2+} homeostasis and cell damage in myopathic skeletal muscle cells. Biochem. Pharmacol. 2005; 70:740–751. [PubMed: 16009351]

47. Solares-Pérez A, Sánchez JA, Zentella-Dehesa A, García MC, Coral-Vázquez RM. Intracellular Ca^{2+} transients in delta-sarcoglycan knockout mouse skeletal muscle. Biochim. Biophys. Acta. 2010; 1800:373–379. [PubMed: 19931597]

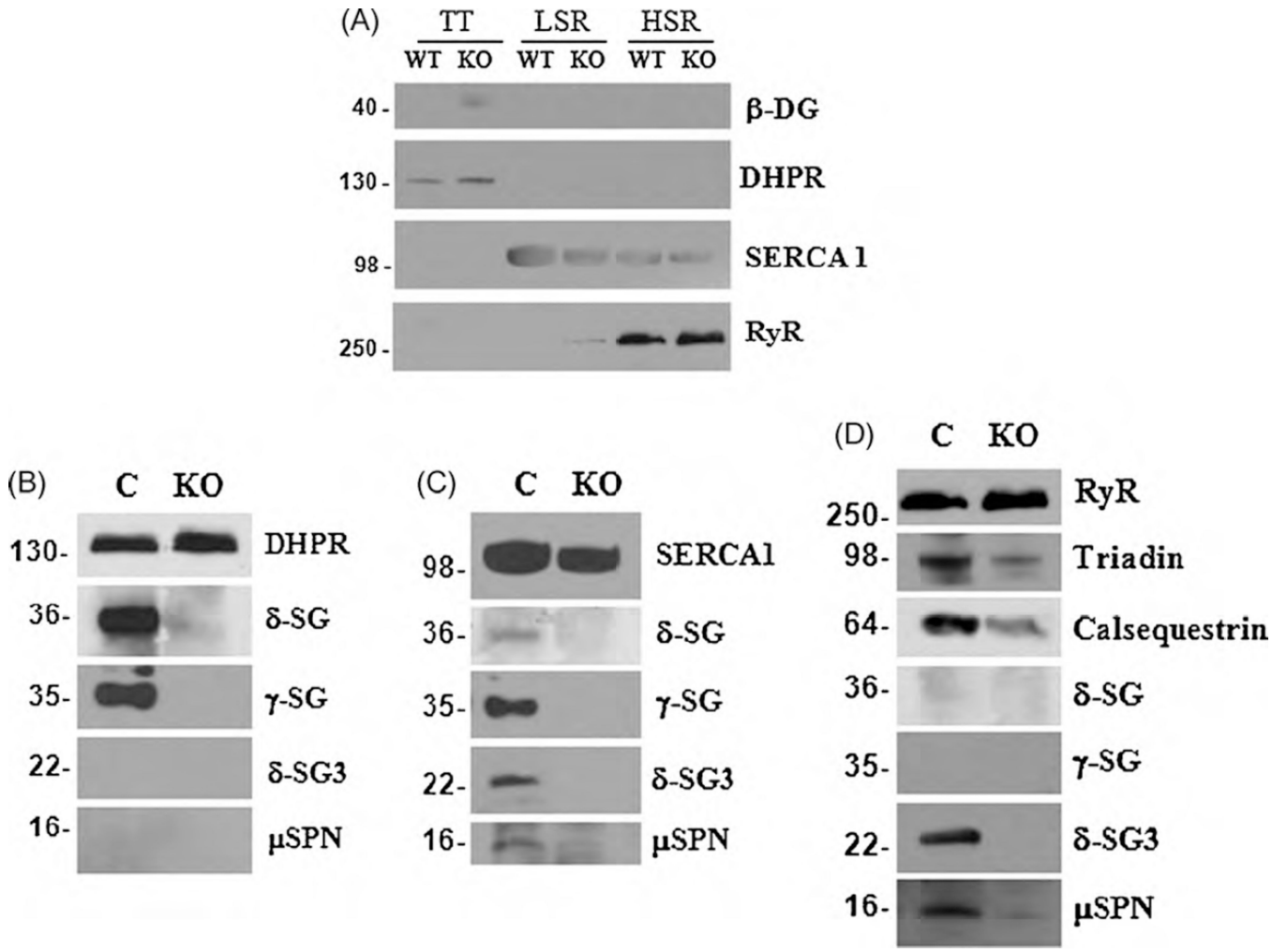

Fig. 1.

Analysis of δ-SG, δ-SG3,γ-SG and μSPN in isolated TT and SR membranes. TT and SR were prepared from skeletal muscle of control and δ-SG KO mice. (A) Immuno-labeling of DHPR, SERCA1 and RyR in different fractions of muscle microsomes after a sucrose gradient preparation. (B) Purified TTs were analyzed by immunoblotting with antibodies to DHPR, δ-SG, γ-SG, δ-SG3 and μSPN. The DHPR is a marker of TT. δ-SG and γ-SG are present in TT of control mice but are absent from TT of dystrophic mice. (C) LSR vesicles were analyzed by immunoblotting to SERCA1, δ-SG, γ-SG, δ-SG3 and μSPN. SERCA1 is enriched in LSR. All the sarcoglycans and μSPN are present in LSR of control mice but are absent from LSR of δ-SG KO mice. (D) HSR vesicles were analyzed by immunoblotting to RyR, triadin, calsequestrin, δ-SG, γ-SG, δ-SG3 and μSPN. RyR, triadin and calsequestrin are found in HSR. Triadin and calsequestrin appear somewhat decreased in δ-SG KO mice. δ-SG3 and μSPN are present in HSR of control mice but are absent from HSR of dystrophic mice.

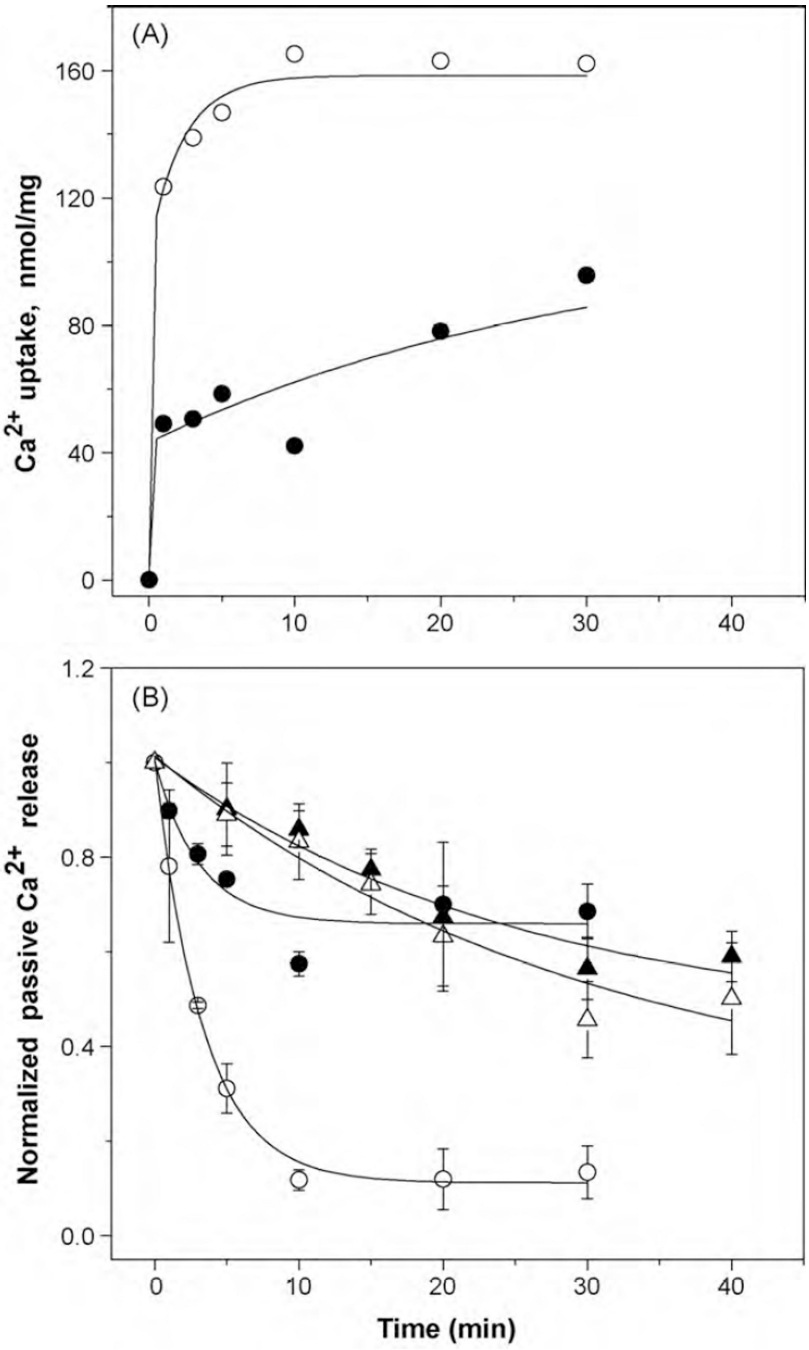

Fig. 2.

ATP-dependent Ca^{2+} transport and passive Ca^{2+} efflux in LSR vesicles obtained from control and δ-SG KO mice as a function of time. Experiments performed with vesicles isolated from control (●) and δ-SG KO (○) animals, respectively. (A) ATP-dependent Ca^{2+} transport from 0.15 mg/ml LSR vesicle aliquots was measured in a solution containing the following: (in mM) 100 KCl, 5 $MgCl_2$, 0.1 $CaCl_2$, 1 μMCi/ml [$^{45}CaCl_2$], 5 mM K-oxalate and 4 ATP, 20 Tris–malate (pH 7.0). (B) Passive Ca^{2+} efflux was determined in the absence of K-oxalate. Aliquots of LSR of 0.3 mg/ml vesicles were incubated in a solution containing

the following: (in mM) 0.1 $CaCl_2$, 5 $MgCl_2$, 100 KCl, 20 Tris–malate, 1 Mg-ATP, 1 μCi [$^{45}CaCl_2$] (pH 7.0) and 2.5 μM in the presence of thapsigargin (▲) for control and (△) δ-SG KO mice. Passive Ca^{2+} efflux was normalized to the maximum transport activity measured 30 min before the beginning of the reaction. Continuous line, best fit to the experimental points.

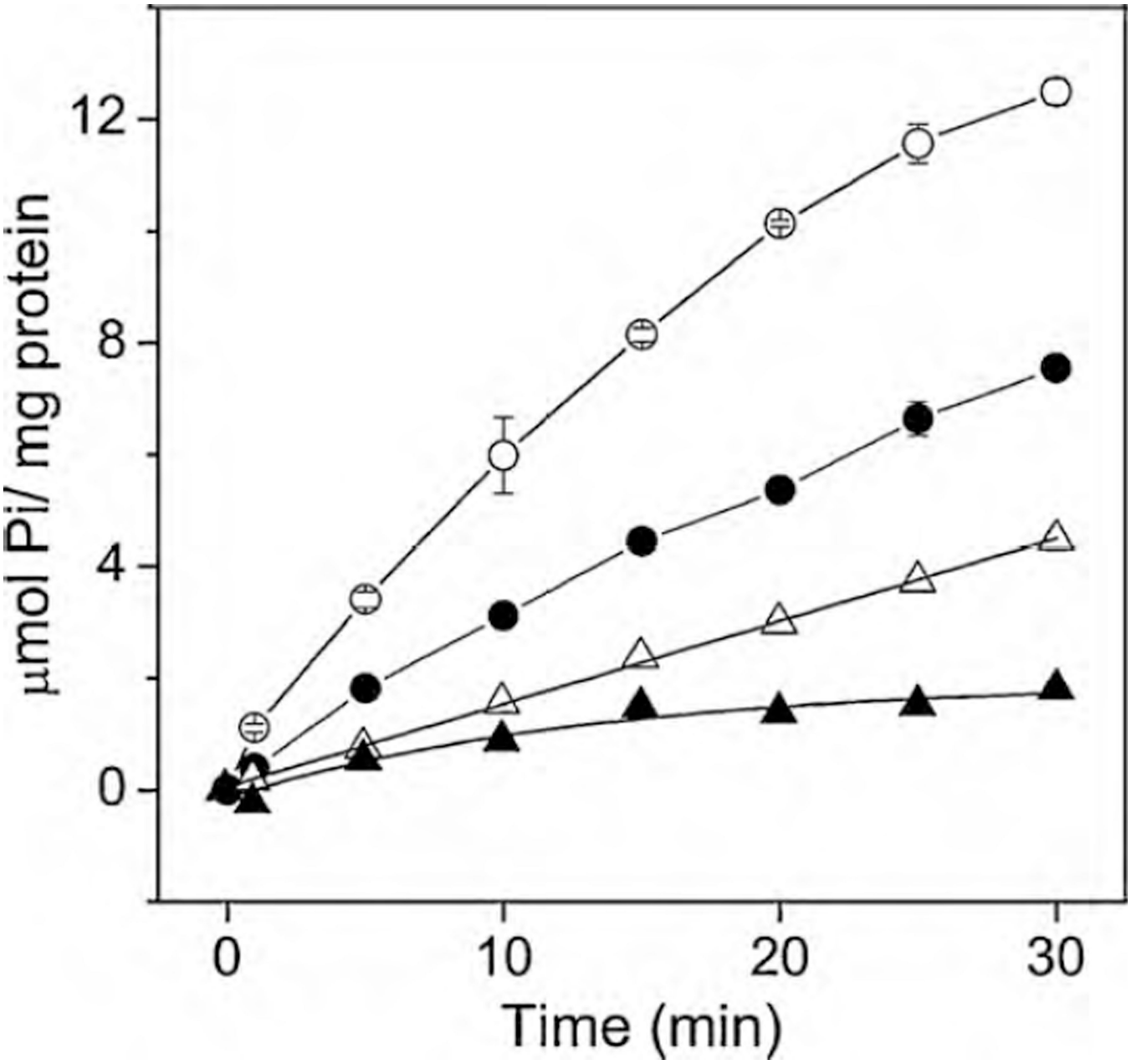

Fig. 3.

Ca^{2+} pump hydrolytic activity of isolated LSR vesicles from control and δ-SG KO mice as a function of time. Experiments performed with vesicles isolated from control (●) and δ-SG KO (○) animals, respectively. Ca^{2+} pump activities were measured from 0.005 mg/ml in a solution containing the following: (in mM) 100 KCl, 5 $MgCl_2$, 1 ouabain, 0.1 $CaCl_2$, 5 NaN_3, 0.33 ATP, and 20 Tris–malate (pH 7.0) and in the presence of 0.5 µM of thapsigargin (▲) for control and (△) δ-SG KO mice. Hydrolytic activity at 30 min was 7.64 and 12.42 µmol/mg from control and dystrophic animals, respectively. Continuous line, best fit to the experimental points.

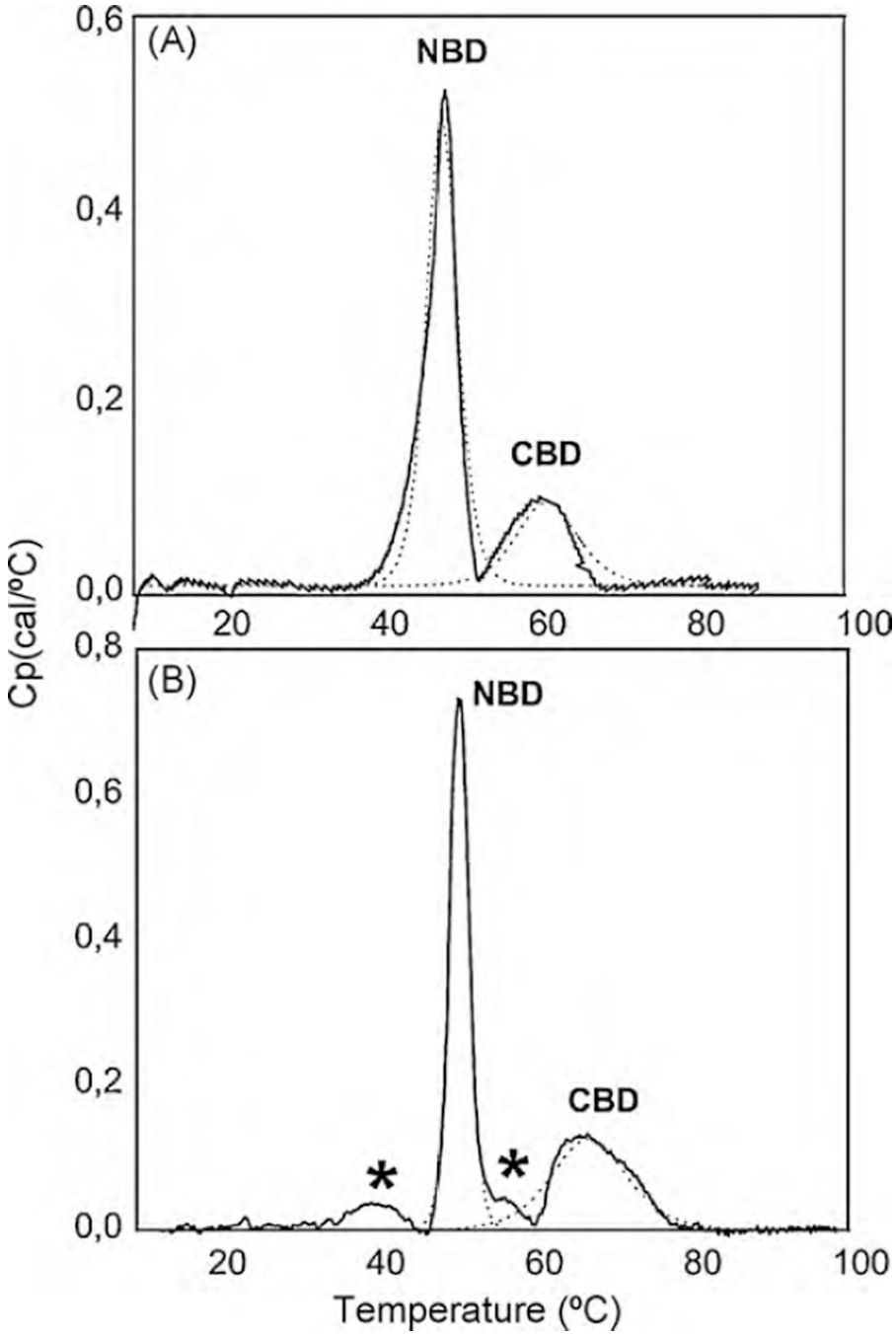

Fig. 4.

Differential scanning calorimetric profiles (Cp vs. temperature) of (A) LSR isolated from control animals and (B) LSR membranes isolated from dystrophic animals. LSR membranes (0.5 mg/ml) were scanned with temperature increasing at a rate of 1°C/min in a solution containing 10% sucrose, 1 mM DTT, 20 mM Tris–malate, and 1 mM $CaCl_2$, pH 7.0. Solid line represents the experimental data, and the best theoretical fit is represented by the dotted line. *Peak NBD* is the nucleotide-binding domain, *peak CBD* is the Ca^{2+}-binding domain and *peak labeled with asterisks* are undetermined structural domains.

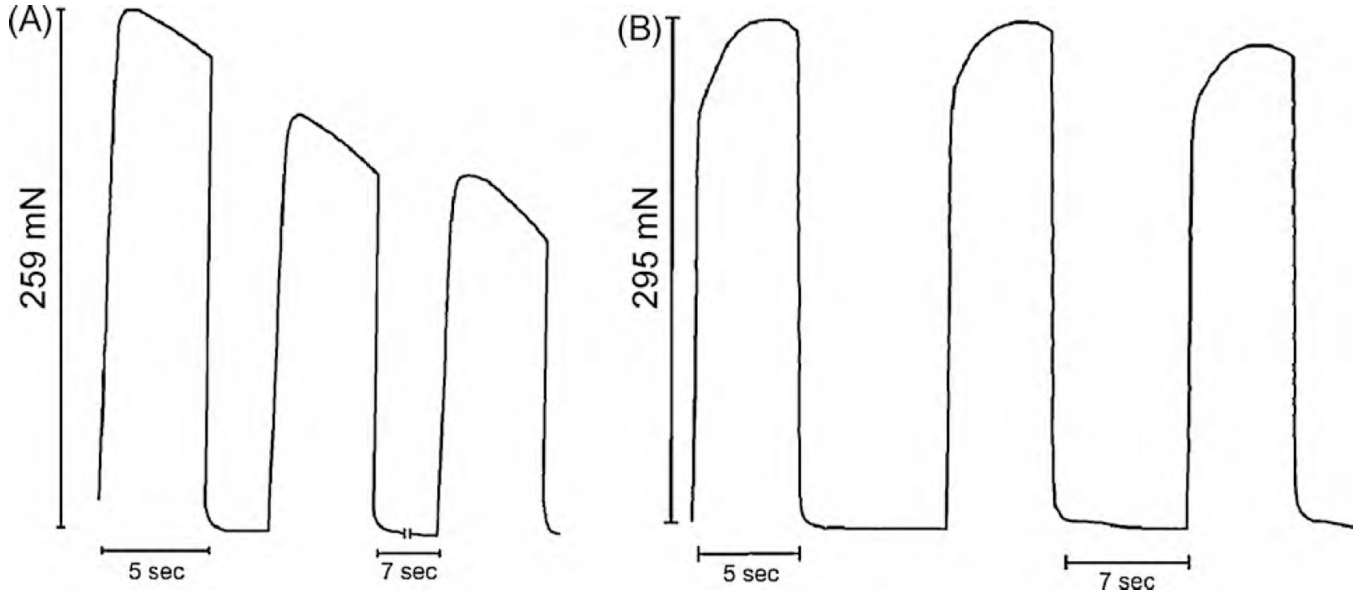

Fig. 5.

Mechanical properties of δ-SG KO *extensor digitorum longus* (EDL). Tetanic stimulation with a protocol of three consecutive electrical stimulation cycles of 75 Hz, 100 V and 5 s with a 7-s rest on (A) WT EDL muscle and (B) δ-SG KO EDL muscle. The contractile machinery functions normally and force generation is 259 mN in WT and 295 mN in δ-SG KO EDL. The muscle cross-section is 1.84 ± 0.403 mm (WT) and 1.9 ± 0.39 mm (δ-SG KO) EDL; $n = 4$ (±SD).

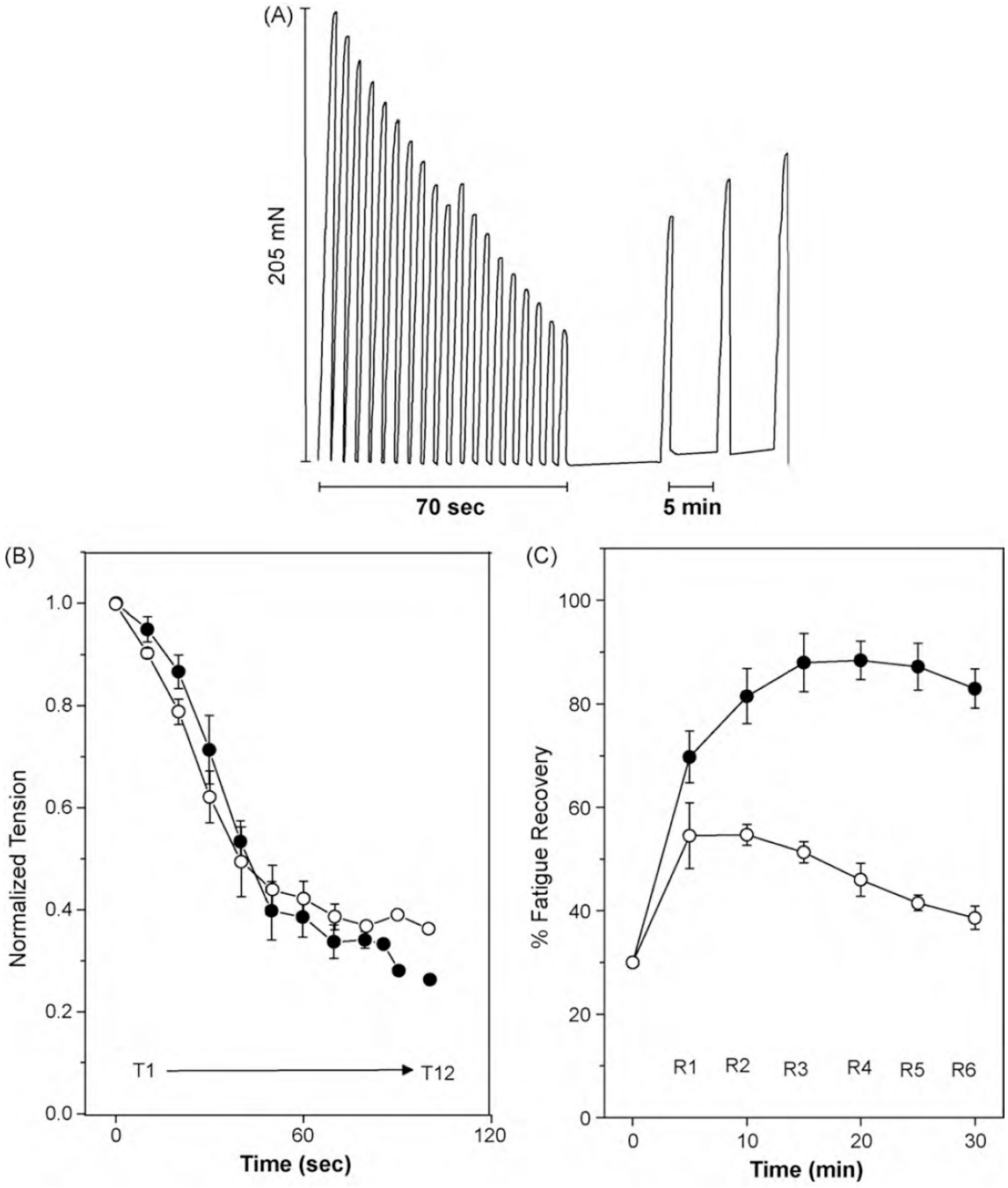

Fig. 6.

Fatigue development and recovery in the δ-SG KO *extensor digitorum longus* (EDL). (A) Representative experiment of fatigue protocol obtained with a 0.6-s long train of tetanic stimulations at 75 Hz, 100 V applied over a period of 70s and the recovery of force after rest with the same stimulation protocol. (B) Normalized force obtained from the fatigue experiment for WT (●) and for δ-SG KO (○) ($n = 3$). A 70% loss of force in both muscles was achieved at the same time (70s) with a final force of 77 mN for WT and 67 mN for δ-SG KO. T1–T12 are the numbers of tetanic stimulation. (C) Percentage recovery after the

fatigue protocol with 5-min rest intervals between stimulations for WT (●) and δ-SG KO (○) ($n = 3$). R1-R6 are the number of tetanic stimulation after the fatigue protocol.

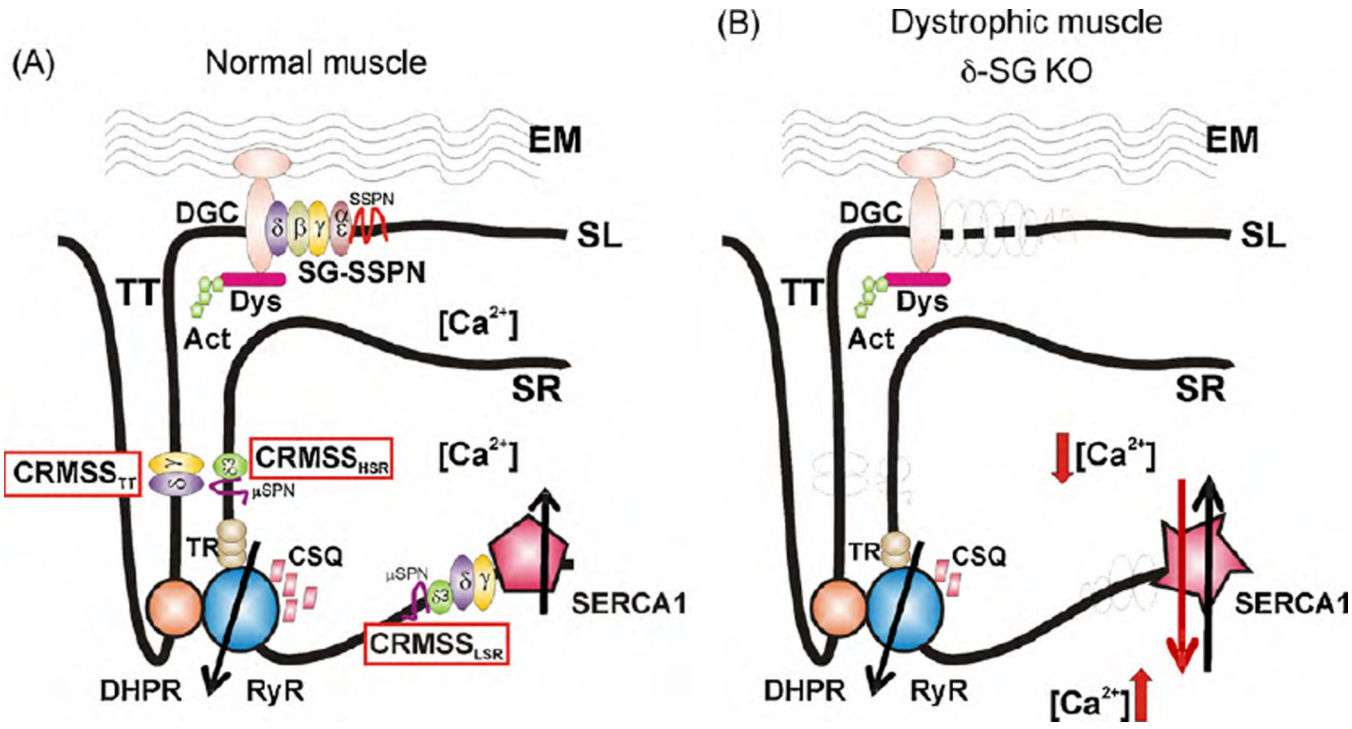

Fig. 7.

Model of the possible involvement of the CRM SG-SSPN (CRMSS) complex in the pathogenesis of muscular dystrophy. The schematic diagram illustrates differences in Ca^{2+} handling within WT (A) and dystrophic (B) skeletal muscle fibers. The primary deficiency of δ-SG leads to the absence of the SG-SSPN subcomplex (SG-SSPN) in sarcolemma (SL), which stabilizes the dystrophin-glycoprotein complex (DGC) that protects against contraction-induced damage. Influx of calcium ions leads to elevated cytosolic Ca^{2+} below the sarcolemma causing increased Ca^{2+}-dependent proteolysis. Based on the evidence presented in this report, we also found that in the case of the CRMs [transverse tubules (TT) and sarcoplasmic reticulum (SR)], the primary deficiency of δ-SG leads to the absence of CRMSS complex. The CRMSS complex is composed of δ-SG isoforms, γ-SG and μSPN, but the combination varies with distinct membrane subfractions. For this reason we propose subtypes of the complex ($CRMSS_{TT}$, $CRMSS_{LSR}$ and $CRMSS_{HSR}$). In the case of dystrophic animals, absence of the $CRMSS_{LSR}$ complex affects the structure and function of SERCA1, suggesting that this may be another source that causes Ca^{2+} mishandling and contributes to the pathogenesis of muscular dystrophy. Triadin (TR) and calsequestrin (CSQ) appear slightly decreased in δ-SG KO mice compared to control levels. Also indicated in the model are extracellular matrix (EM), dystrophin (Dys), actin cytoskeleton (Act), dihydropyridine receptor (DHPR) and ryanodine receptor (RyR).